Supporting Information

Gill et al. 10.1073/pnas.1305269110

SI Materials and Methods

Immunofluorescence Imaging. Cells were seeded at desired densities onto glass coverslips in 24-well dishes (Nunc) or 96-well black imaging plates (BD Falcon) and incubated for 24–48 h. Treatment of cells with the Src inhibitor, PP2, and transient expression of Arf1-GFP plasmids were performed as outlined previously (30). For total cell immunofluorescence staining, cells were washed for 10 min with D-PBS, fixed for 10 min using 4% paraformaldehyde in D-PBS, washed for a further 10 min with D-PBS, and permeabilized with 0.2% Triton X-100 in D-PBS for 5 min. Cells were then blocked for 10 min each with 2% FBS in D-PBS before antibody staining. For cell surface staining, the same procedure was followed except for the use of Triton permeabilization. Primary antibodies used include: mouse anti-GalNAc-T1 and -T2 hybridoma (1:2, a gift from H.C.), rabbit anti-Giantin (ab24586, 1:1,000; Abcam), rabbit anti-GM130 (#610822, 1:300; BD Biosciences), mouse anti-PDI (ab2792, 1:300; Abcam), chicken anti-Calreticulin (ab14234, 1:300; Abcam), goat anti-FISH/Tks5 (ab118575, 1:300; Abcam), rabbit anti-FAK (ab40794, 1:300; Abcam), rabbit anti-FAK(Y861P) (ab4804, 1:300; Abcam), mouse anti-Paxillin (ab3127, 1:300; Abcam), rabbit anti-Paxillin (Y31P) (ab32115, 1:300; Abcam), rabbit anti-cSrc (sc18, 1:50; Santa Cruz Biotechnology), and rabbit anti-Actin (ab15263, 1:300; Abcam). Secondary staining with species appropriate Alexa Fluor-conjugated antibodies (1:400; Invitrogen) or cy5-conjugated HPL (L32454, 2 μg/mL; Invitrogen) and biotin-conjugated VVL (B1075, 4 μg/mL; Vector Laboratories) or PNA (B1235, 10 μg/mL; Vector Laboratories) lectins, and Hoesct (1:10,000 Invitrogen) was performed for 1–3 h following the manufacturer's instructions. Biotin-conjugated VVL or PNA was further stained with Streptavidin-Alexa594 (S11227, 1:400; Invitrogen) for 1 h. Coverslips were mounted using Fluorsave (Millipore) and left to dry overnight. Cells were imaged either using an Olympus inverted fluoview confocal microscope (model IX81) coupled with a CCD camera (model FVII) with a 100× objective (UPLSAPO; 100×; N.A. 1.4) or Olympus upright fluoview confocal microscope (model BX61) coupled with a CCD camera (model FVII) with a 100× objective (PLAPO; 100×; N.A. 1.45) under immersol oil (Olympus Optical). Images were acquired and processed using Olympus FV10-ASW software. For high-throughput automated imaging experiments, cells were imaged under constant acquisition parameters using high-throughput ImageXpressMICRO widefield microscope with a 10× Plan Fluor objective (Molecular Devices). Typically, four to six sites containing between 50 and 500 cells per site from at least three independent wells per sample were acquired. Image processing and analysis was performed using MetaXpress 3.1 software (Molecular Devices). In experiments where staining intensities were quantified, an intensity-based cutoff was manually selected using the TransfluorHT module to generate an integrated pixel intensity per channel per site. In parallel, the TransfluorHT module was used to quantify cell number (via Hoescht staining) per site. Next, integrated pixel intensity per cell per site was calculated before the mean and SEs for all sites were generated. Finally, the mean integrated intensities per cell were normalized to a manually chosen reference sample (stated for each experiment). In experiments where only cell number were quantified (cell-adhesion experiments), total cells per site were detected (via Hoescht staining) using the Cell Proliferation HT module before the mean and SE for all sites were calculated.

Statistical Analysis. Data are presented as the mean ± SEM. Statistical significance was calculated using one-way ANOVA with Tukey's test for datasets with $n > 2$ samples. In case of $n = 2$ samples, unpaired, two-tailed t tests were used (noted in the respective figure legends). Pearson correlation coefficients (PCCs) were calculated using Olympus FV10-ASW software using high-quality immunofluorescence images acquired at 100× magnification. Nonspecific background fluorescence was removed before PCC calculation. Mean and SEM for calculated MPCC values were determined from three independent images per experiment (resulting in the PCC analysis summarizing the staining results from 10 to 50 cells). Mean Tn staining in the Golgi apparatus of BT549 cells [after Src inhibition or Arf1(Q71L)-GFP expression] was quantified using Olympus FV10-ASW software after drawing a Golgi-localized ROI (delineated by GM130 antibody labeling). Thirty cells (from several independent images) were quantified per sample. VVL staining in FISH/Tks5-positive lamellipodia was quantified using Olympus FV10 after drawing a lamellipodia-localized region of interest (delineated by FISH antibody labeling). Cells from 10 independent images (summarizing >30 separate lamellipodia) were quantified per sample.

Human Tumor Microarray Imaging. Human tumor microarrays (BR2082, MC616 and T087A) were purchased from Biomax. Core identification (e.g., normal, malignant) as well as carcinoma grade and stage classifications were performed by Biomax. See www.biomax.us/tissue-arrays/Breast/BR2082, www.biomax.us/tissue-arrays/Multiple_Organ/MC616, and www.biomax.us/tissue-arrays/Breast/T087a for details on tumor core classification and H&E-stained images of the tumor cores. Samples were deparaffinized (xylene) and rehydrated before antigen retrieval using sodium citrate, pH 6.0 at 60 °C. Neuraminidase- (from *Clostridium perfringens*) (Sigma, N3001) treated samples were incubated with 0.2 mg/mL enzyme in 50 mM sodium citrate (pH 6.0, room temperature), 100 mM NaCl, and 100 μg/mL BSA for 1 h at room temperature. Subsequent staining with VVL-biotin (4 μg/mL) or PNA-biotin (20 μg/mL) and Hoescht (1:10,000) was performed overnight before visualization using Streptavidin-Alexa594 (1:400) for 30 min. Arrays were first automatically imaged (using constant acquisition parameters) using a 10× objective (LD Plan-NEOFLUAR; 10×; N.A. 0.4) on a motorized stage coupled to a Zeiss inverted confocal microscope equipped with a CCD camera (AxioCam HRc). Highest-quality images of the cores were exported as .png files from Zeiss Zen2011 software to enable quantification of lectin staining in tumor cores and adjacent regions (e.g., Fig. 3*B*) using Olympus FV10-ASW software. The integrated intensity of all pixels in tumor cores on equivalently sized background regions were calculated to enable a final intensity per core to be generated by subtraction of nonspecific background fluorescence. Corrected intensities were divided by the core area to generate the intensity per pixel per core. Final normalization to mean intensity per pixel per core from all normal tissue cores in each array was performed to enable direct comparison of VVL and PNA staining in the BR2082 and MC616 arrays. High Tn cores (>threefold versus normal tissue cores) were later imaged using a 100× objective mounted on an Olympus fluoview confocal microscope as outlined above to judge Tn staining patterns by eye. The T087A array was costained with VVL and rabbit anti-Calnexin (ab22595), PNA and rabbit anti-Calnexin, and rabbit anti-Calnexin with chicken anti-Calreticulin (ab14234) to establish baselines for MPCC analysis. The BR2082 array was also costained with VVL and rabbit anti-Calnexin (ab22595). Secondary staining was per-

formed as outlined above. All cores in the small T087A array and 25 randomly acquired high Tn cores (>threefold versus normal tissue cores identified from 10× quantification) from the BR2082 array were imaged at 100× objective mounted on an Olympus fluoview confocal microscope as outlined above. At least three fields per cores corresponding to 15–25 cells were used to measure MPCCs, which were calculated as outlined earlier. For histological samples containing only a few cells with high Tn staining (e.g., Fig. 3*E*, BR2082 core C2), only these cells were included for MPCC analysis.

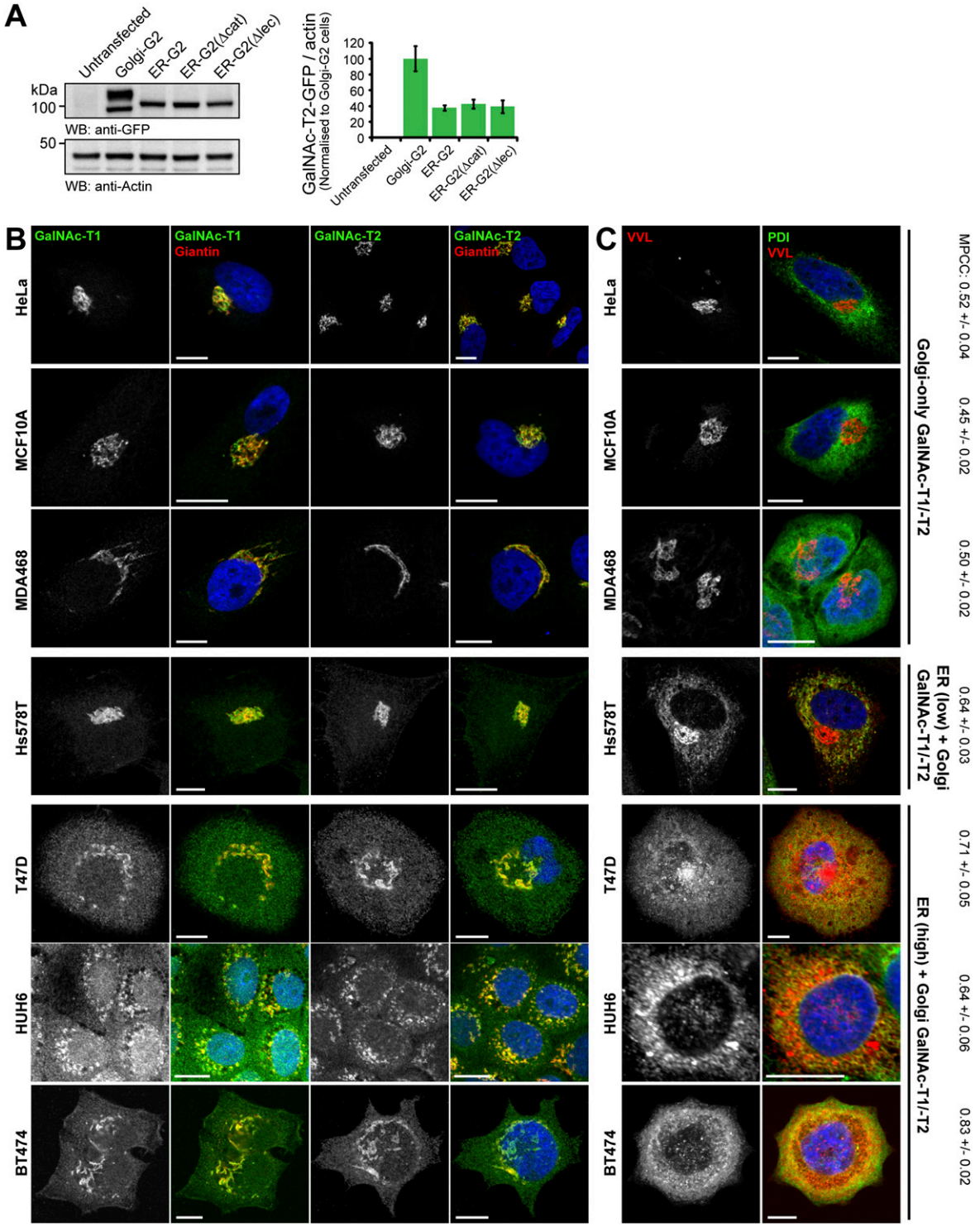

Fig. S1. Model cancer cell lines contain constitutively endoplasmic reticulum (ER)-localized polypeptide *N*-acetylgalactosamine transferase (GalNAc-T1) and -T2. (*A*) Western blot analysis of MDA-231 cells stably expressing GalNAc-T2-GFP constructs. Quantification of GFP levels (relative to actin levels) was performed using ImageJ. Data are represented as mean ± SEM normalized to Golgi-G2 cells ($n = 2$ experiments). (*B*) GalNAc-T1 and -T2 staining in cancer cell lines along with the Golgi marker Giantin. (*C*) High Tn staining (*Vicia villosa* agglutinin B4 lectin, VVL) colocalizes with the ER-marker protein disulphide isomerase (PDI) in cancer cell lines with ER-localized GalNAc-T1/-T2. MPCC, mean Pearson correlation coefficient between VVL and PDI labels ($n = 3$ images). MPCC for poorly colocalized PDI (ER) and Giantin (Golgi) labels ($n = 3$ images) are 0.55 ± 0.01 (HeLa), 0.25 ± 0.02 (MDA231), 0.28 ± 0.02 (MCF10A), 0.43 ± 0.01 (MDA468), 0.23 ± 0.03 (Hs578T), 0.44 ± 0.04 (T47D), 0.54 ± 0.06 (BT474), 0.32 ± 0.02 (BT549), and 0.34 ± 0.06 (HUH6). Nuclei stained using Hoechst. (Scale bars, 10 μm.)

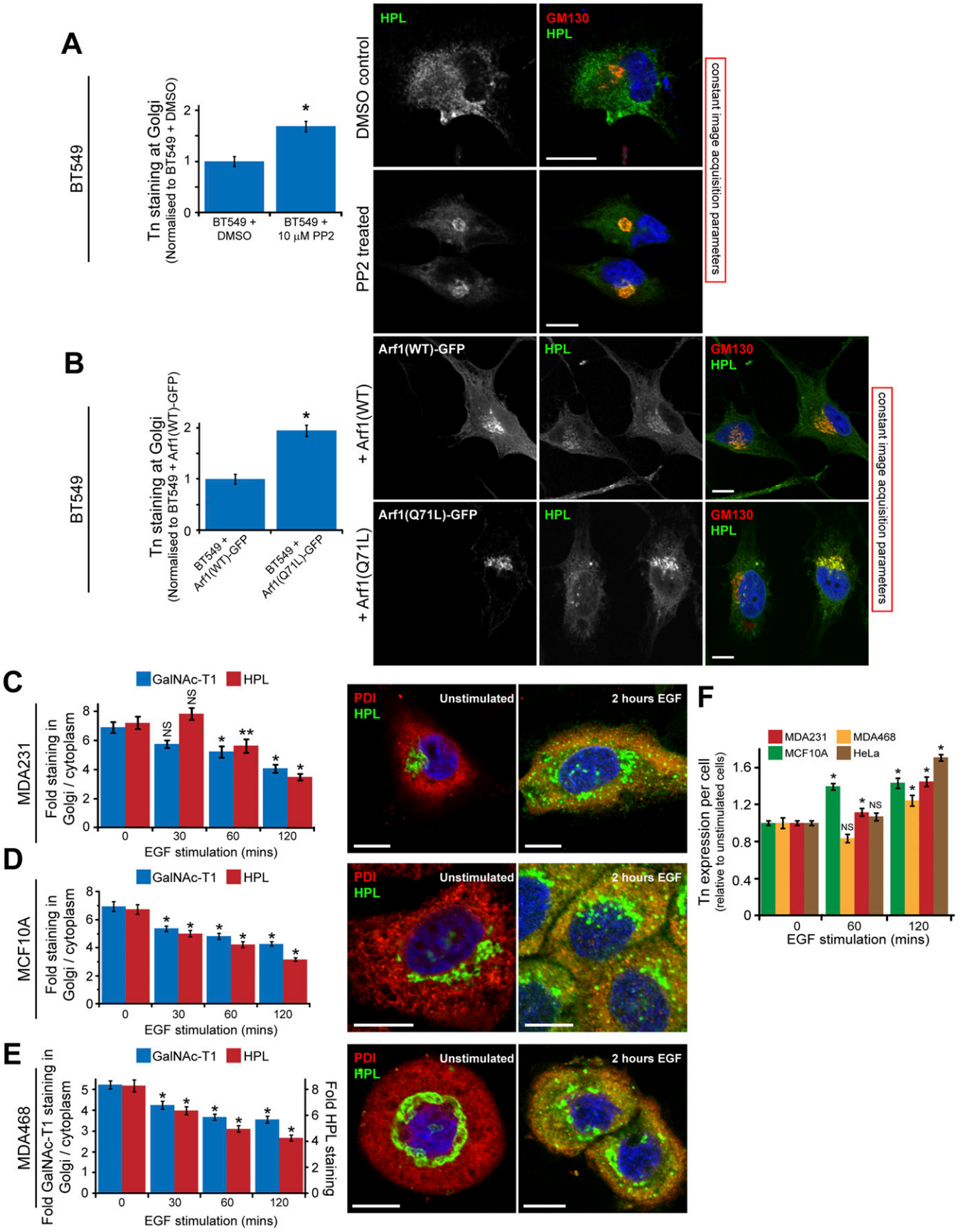

Fig. S2. EGF stimulation promotes specific relocation of GalNAc-Ts in cancer cells with Golgi-localized GalNAc-Ts. (*A*) Tn staining in the Golgi ± SEM in BT549 cells treated overnight with DMSO or the Src inhibitor, PP2 (10 μM). Tn staining in Golgi (delineated by GM130 labeling) was quantified for 30 cells in each

Legend continued on following page

sample. *$P < 0.01$ relative to DMSO-treated cells (*t* test). (*B*) Tn staining in the Golgi ± SEM in BT549 cells transiently expressing Arf1(WT)-GFP or Arf1(Q71L)-GFP. Tn staining in Golgi (delineated by GM130 labeling) was quantified for 30 cells in each sample. *$P < 0.01$ relative to DMSO-treated cells (*t* test). (*D* and *E*) Ratio of GalNAc-T1 and *Helix pomatia* lectin (HPL) staining in the Golgi apparatus (marked by Giantin labeling) relative to the surrounding cytoplasm in MDA231 (*C*), MCF10A (*D*), and MDA468 (*E*) cancer cells before and after EGF (100 ng/mL) stimulation. Quantification was performed as outlined previously (1). *$P < 0.01$, **$P < 0.05$ relative to untreated cells (0 min EGF). Costaining for Tn (marked with HPL) and the ER marker PDI before and after 2 h EGF stimulation is also shown. (*F*) Mean of Tn expression ± SEM in model cancer cells before and after EGF stimulation (100 ng/mL) for 2 h. *$P < 0.01$ relative to unstimulated cells. Nuclei stained using Hoechst. (Scale bars, 10 μm.)

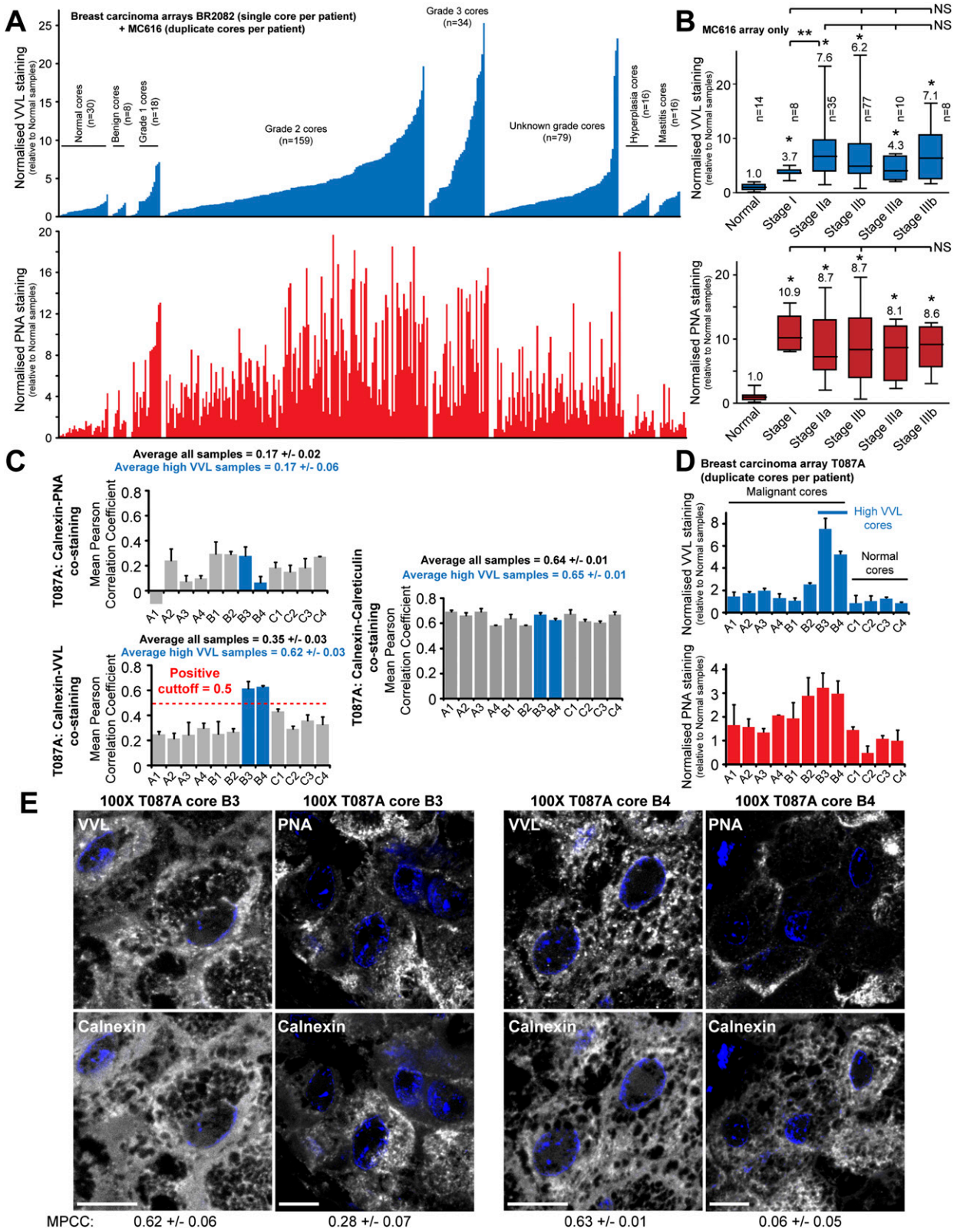

Fig. S3. Tn- and T-antigen expression in human breast cancer microarrays. (*A*) Ranked VVL and corresponding peanut agglutinin (PNA) staining intensities in prearrayed paraffin-embedded tumor tissue cores from BR2082 and MC616 human breast cancer microarrays. VVL and PNA intensities are listed in Table S2. (*B*) Quantification of Tn and T staining in human breast cancer biopsies from the MC616 array. $*P < 0.01$ and $**P < 0.05$ relative to normal tissue cores (Mann–Whitney). NS, not significant. Histological stage confirmed by pathologist. (*C*) Colocalization analysis of different marker combinations in the T087A human breast cancer microarray. Three independent images acquired at 100× magnification were used to calculate MPCC values. (*D*) Ranked VVL and corresponding PNA staining intensities in tissue cores from the T087A human breast cancer microarray. (*E*) Costaining Calnexin-VVL and Calnexin-PNA in high Tn Cores from the T087A array. Tn staining colocalizes well with Calnexin to generate high MPCC values. PNA staining, that is predominately localized at the cell surface, colocalizes poorly with Calnexin to generate low MPCC values. (Scale bars, 10 μm.) Nuclei stained using Hoechst.

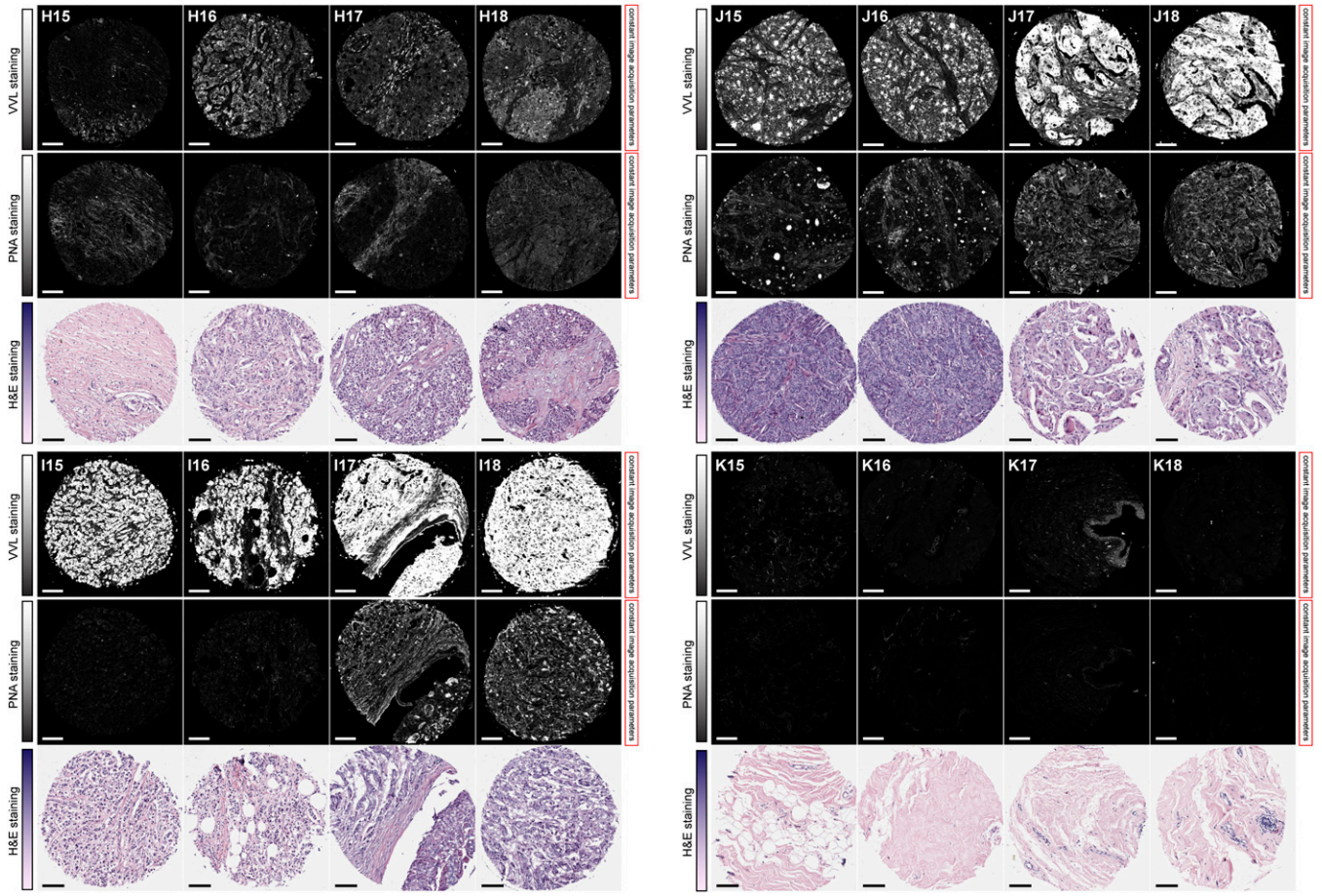

Fig. S4. Example images of Tn-antigen (VVL), T-antigen (PNA), and H&E staining in malignant breast carcinoma cores (H15–H18, I15–I18, J15–J18) or normal breast tissue cores (K15–K18) from the MC616 array. H&E images are used with permission from Biomax (www.biomax.us/tissue-arrays/Multiple_Organ/MC616). (Scale bars, 100 μm.)

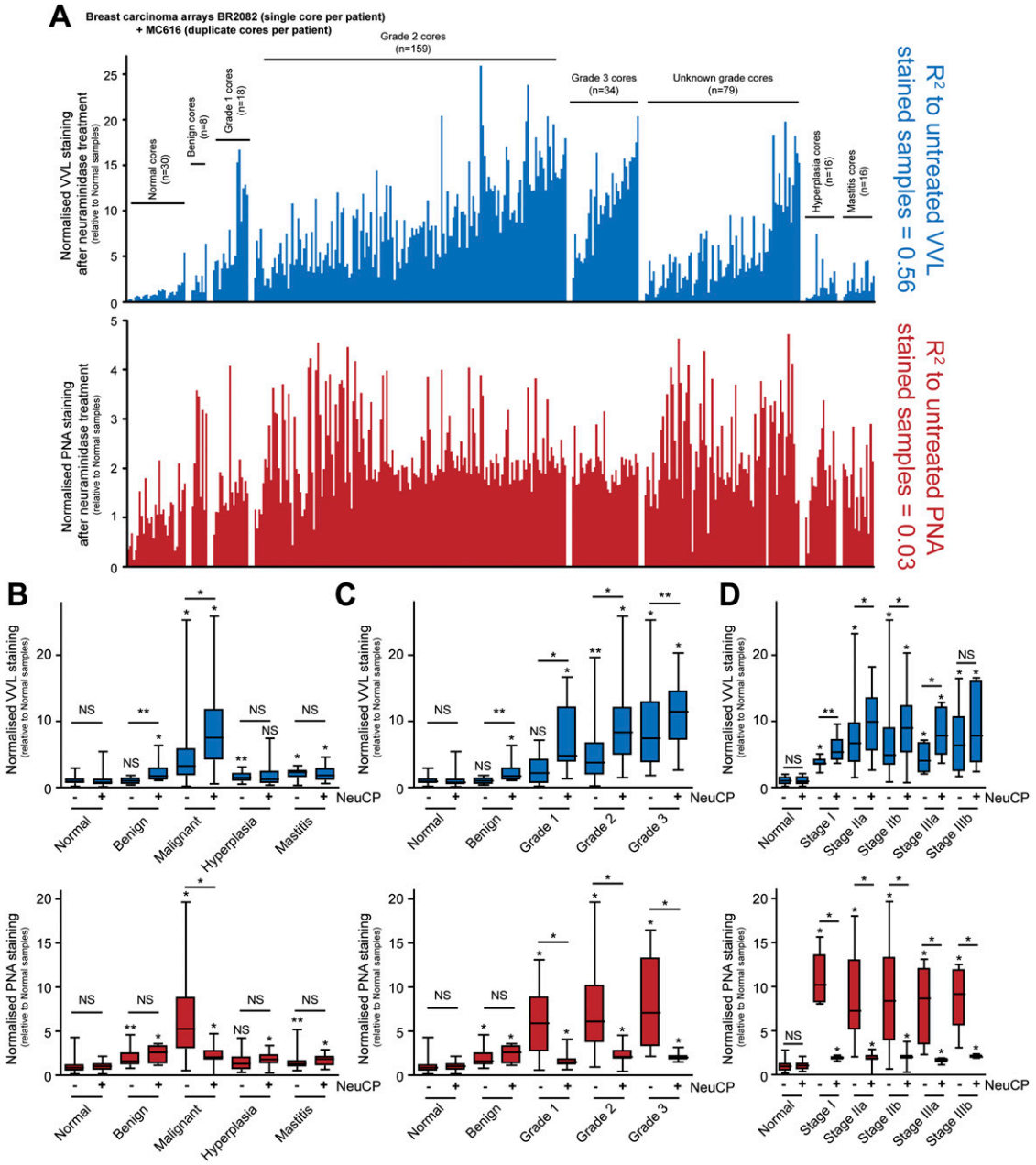

Fig. S5. Tn- and T-antigen expression in human breast cancer microarrays after neuraminidase treatment to remove terminal sialic acid residues. (*A*) Ranked VVL and corresponding PNA staining intensities in prearrayed paraffin embedded tumor tissue cores from BR2082 and MC616 human breast cancer microarrays after treatment with neuraminidase from *Clostridium perfringens* (NeuCP). Core ranking is as shown previously in Fig. S3*A*. VVL and PNA intensities are listed in Table S2. (*B–D*) Quantification of Tn and T staining human breast cancer biopsies from the BR2082 and MC616 arrays. $*P < 0.01$ and $**P < 0.05$ relative to normal tissue cores or indicated samples (Mann–Whitney). NS, not significant. Histological grade (*C*) and stage (*D*) confirmed by pathologist.

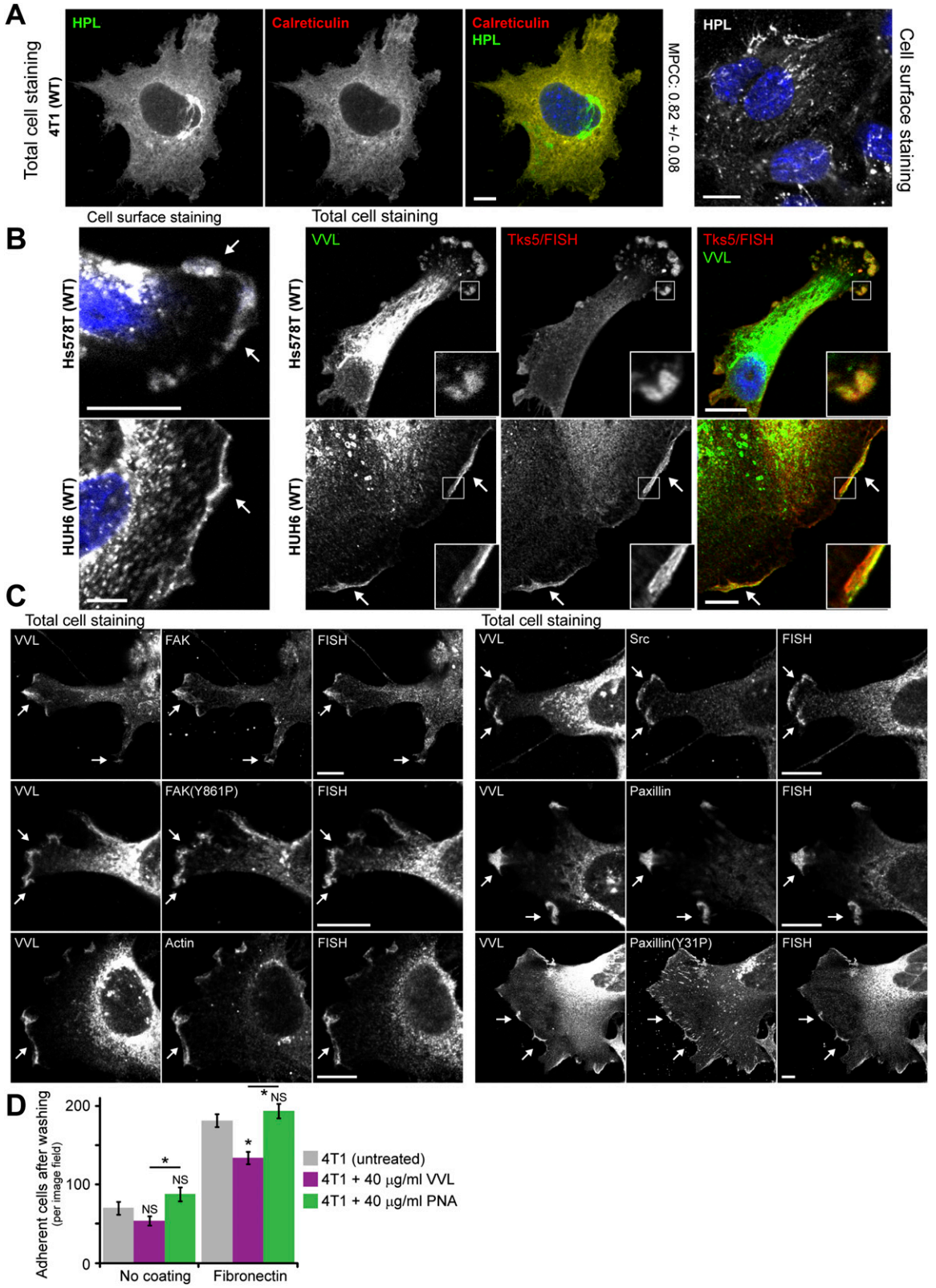

Fig. S6. Tn-bearing cell surface proteins are enriched in active lamellipodia of 4T1 carcinoma cells containing ER-localized GalNAc-Ts. (*A*) Wild-type 4T1 breast carcinoma cells contain ER-localized GalNAc-Ts activity as judged by abundant colocalization of intracellular Tn staining (HPL) with the ER marker Calreticulin as well as cell surface Tn staining (HPL). (*B*) Costaining Tn (VVL) with the lamellipodia marker Tks5/FISH in Hs578T and HUH6 cells containing ER-localized GalNAc-Ts. (*C*) Costaining Tn (VVL), FISH/Tks5, and various markers of active lamellipodia in 4T1 carcinoma cells with ER-localized GalNAc-Ts. (*D*) Adhesion of 4T1 cells to fibronectin after VVL or PNA preincubation for 20 min. *$P < 0.01$ relative to untreated cells or indicated samples. Nuclei stained using Hoechst. (Scale bars, 10 μm.)

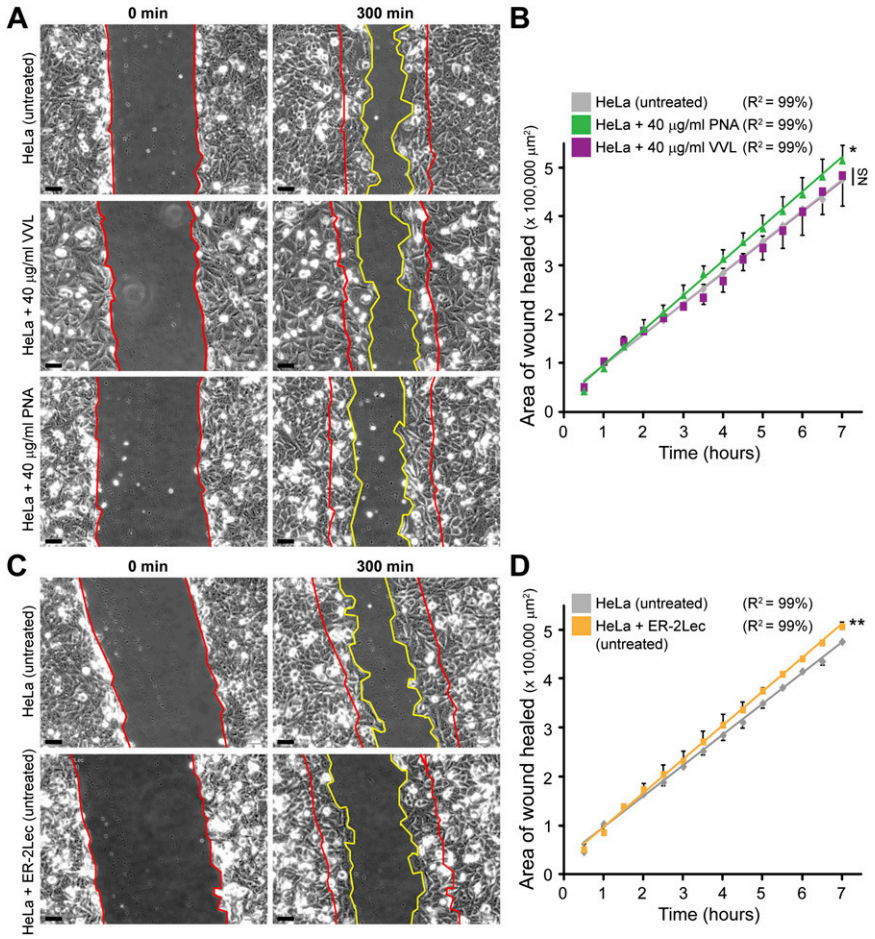

Fig. S7. Effects of exogenous lectin treatment or ER-2Lec expression on HeLa carcinoma cell migration in vitro. (*A*) Wound healing of wild-type HeLa cells on fibronectin after VVL or PNA preincubation for 20 min. (*B*) Mean of wound closure ± SEM ($n = 2$ experiments). *$P < 0.01$ relative to untreated cells. (*C*) Wound healing of HeLa cells expressing ER-2Lec on fibronectin. (*D*) Mean of wound closure ± SEM ($n = 2$ experiments). Untreated experimental samples from Fig. S6B are shown for comparison. *$P < 0.05$ relative to untreated cells. (Scale bars, 100 μm.)

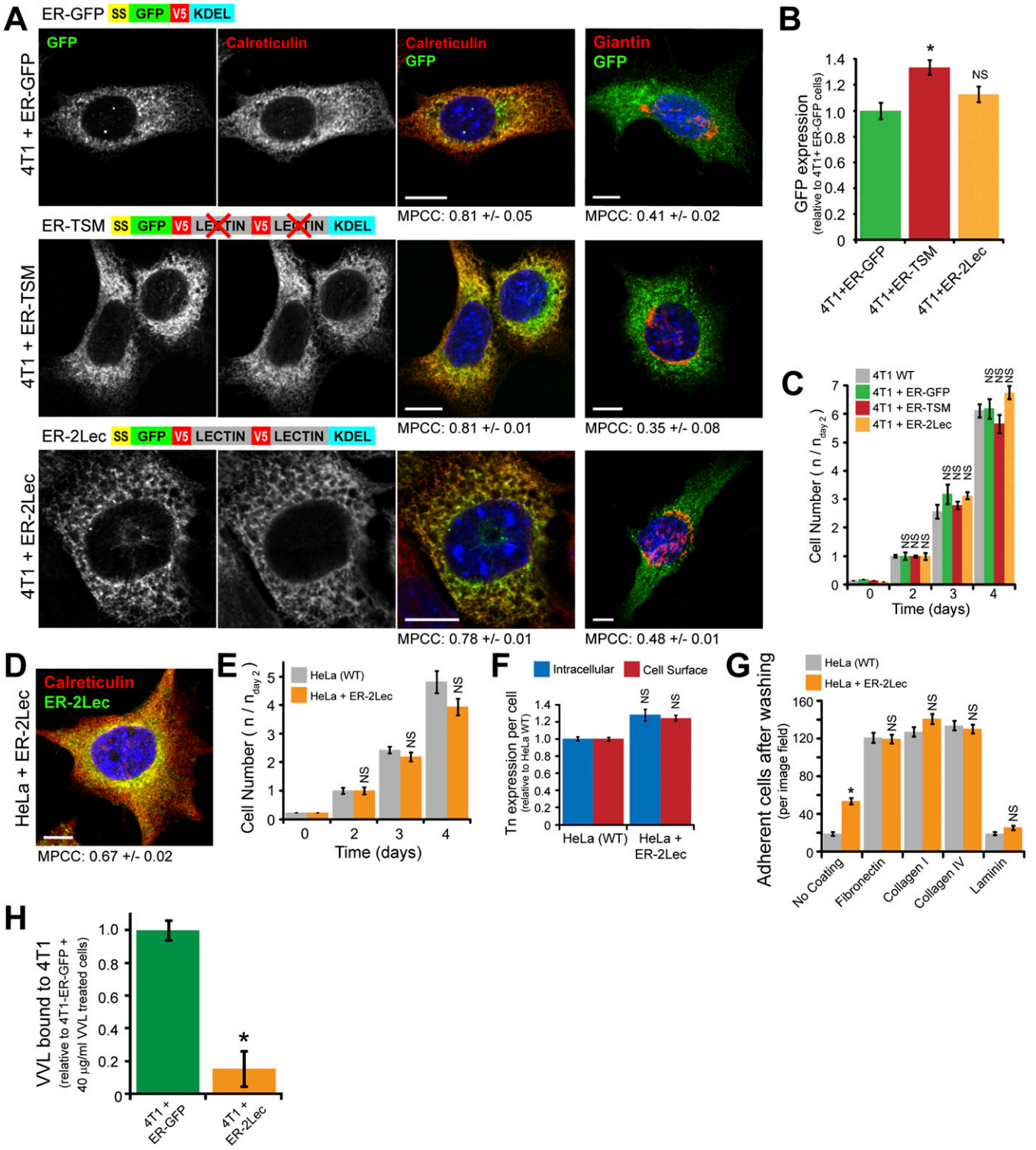

Fig. S8. Effects of ER-GalNAc-Ts inhibitor in 4T1 cells. (*A*) ER-GFP, ER-triple sugar mutant (ER-TSM), and ER-2Lec constructs stably expressed in 4T1 cells extensively colocalize with the ER marker Calreticulin but not the Golgi marker Giantin. MPCC for poorly colocalized Calreticulin (ER) and Giantin (Golgi) labels ($n = 3$ images) are 0.52 ± 0.06 (4T1-ER-GFP), 0.37 ± 0.02 (4T1-ER-TSM), and 0.46 ± 0.03 (4T1-ER-2Lec). (Scale bars, 10 μm.) (*B*) ER-GFP, ER-TSM, and ER-2Lec constructs are homogeneously expressed at a similar level. Data are represented as mean ± SEM normalized to mean fluorescence intensity of 4T1 + ER-GFP cells. NS, not significant. (*C*) Model 4T1 cell lines grow at a similar rate as wild-type cells. Data are represented as mean ± SEM ($n = 6$). (*D*) ER-2Lec construct stably expressed in HeLa cells extensively colocalizes with the ER marker Calreticulin. MPCC between GFP-ER-2Lec and Giantin (Golgi) labels ($n = 3$ images) is 0.44 ± 0.01. (Scale bar, 10 μm.) (*E*) HeLa cells stably expressing ER-2Lec grow at a similar rate as wild-type cells. Data are represented as mean ± SEM ($n = 6$). (*F*) Mean of Tn expression ± SEM in HeLa cells expressing ER-2Lec relative to wild-type cells using high-throughput microscopy. (*G*) Mean of adhesive strength ± SEM of HeLa cells stably expressing ER-2Lec relative to wild-type cells (*t* test). (*H*) VVL bound to adherent 4T1 cells from the experiment shown in Fig. 6*F*. *$P <$ 0.01 (*t* test).

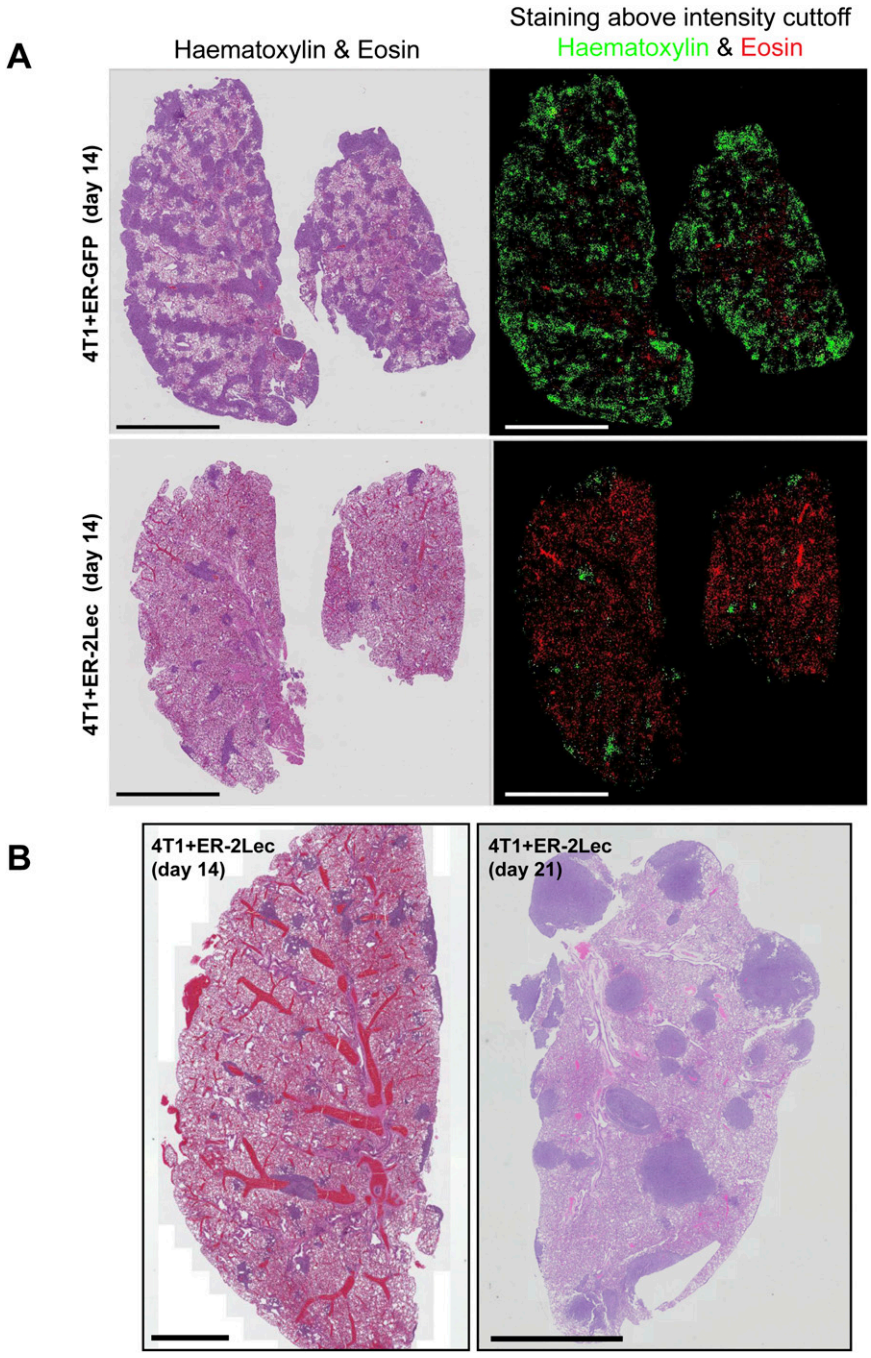

Fig. S9. Effects of ER-GalNAc-Ts inhibitor on metastatic potential of 4T1 cells. (*A*) H&E staining reveals more metastatic nodules (dark purple) in the lung parenchyma of mice injected with 4T1 expressing control construct ER-GFP than in ER-2Lec expressing cells. Quantification of tumor area relative to total using Haematoxilin staining. (*B*) H&E staining of lungs in mice injected with ER-2Lec expressing 4T1 cells at days 14 and 21. Note enlargement of tumors leading to loss of pulmonary function. (Scale bars, 2 mm.)

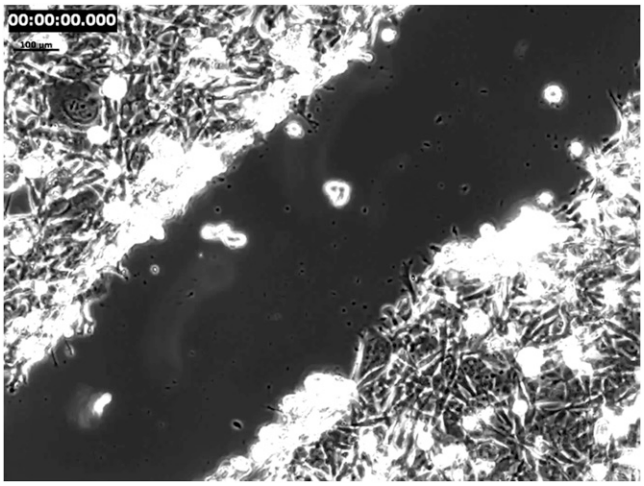

Movie S1. ER-G2 cells (present movie) migrate faster than Golgi-G2 (Movie S2) and untransfected MDA231 (Movie S3) cells into the denuded area of a scratch wound. Frames were acquired at 3-min intervals over a 7-h time period.

Movie S1

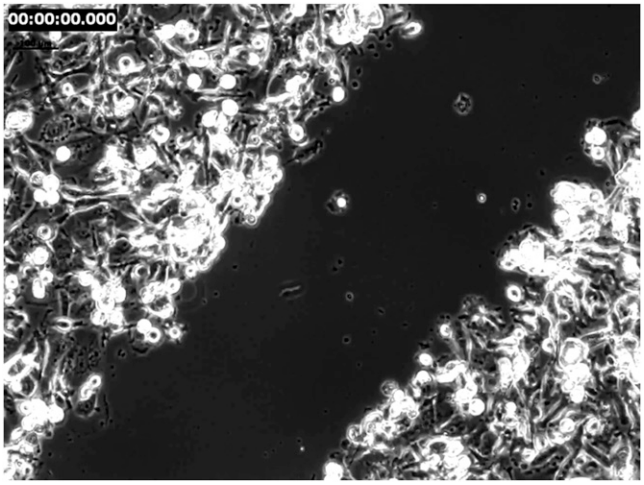

Movie S2. ER-G2 cells (Movie S1) migrate faster than Golgi-G2 (present movie) and untransfected MDA231 (Movie S3) cells into the denuded area of a scratch wound. Frames were acquired at 3-min intervals over a 7-h time period.

Movie S2

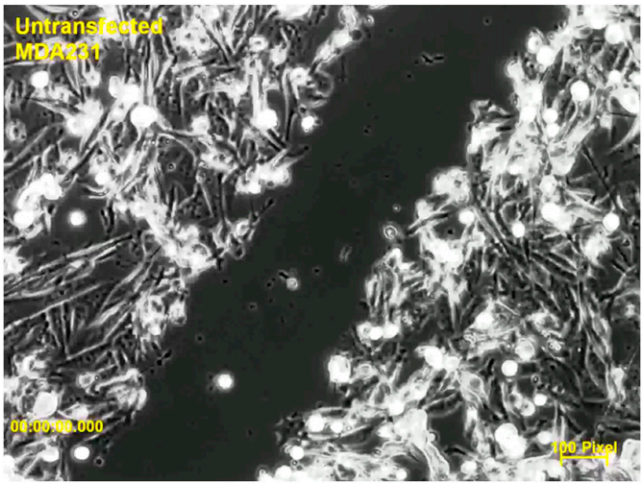

Movie S3. ER-G2 cells (Movie S1) migrate faster than Golgi-G2 (Movie S2) and untransfected MDA231 (present movie) cells into the denuded area of a scratch wound. Frames were acquired at 3-min intervals over a 7-h time period.

Movie S3

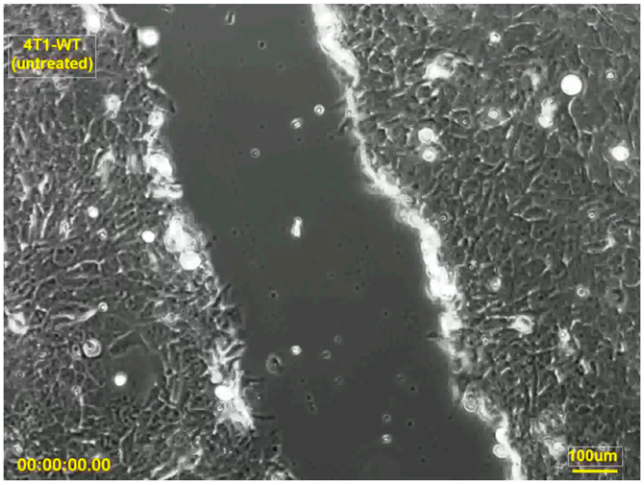

Movie S4. Untreated wild-type 4T1 cells (present movie) migrate faster than 40 μg/mL VVL-treated wild-type 4T1 cells (Movie S5) into the denuded area of a scratch wound. Frames were acquired at 5-min intervals over an 8-h time period.

Movie S4

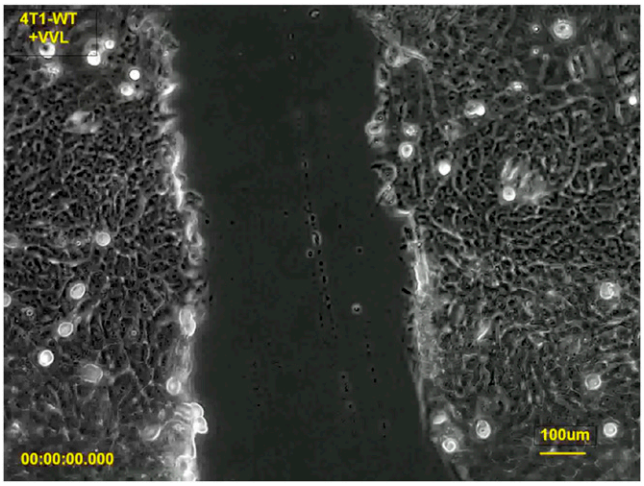

Movie S5. Untreated wild-type 4T1 cells (Movie S4) migrate faster than 40 μg/mL VVL-treated wild-type 4T1 cells (present movie) into the denuded area of a scratch wound. Frames were acquired at 5-min intervals over an 8-h time period.

Movie S5

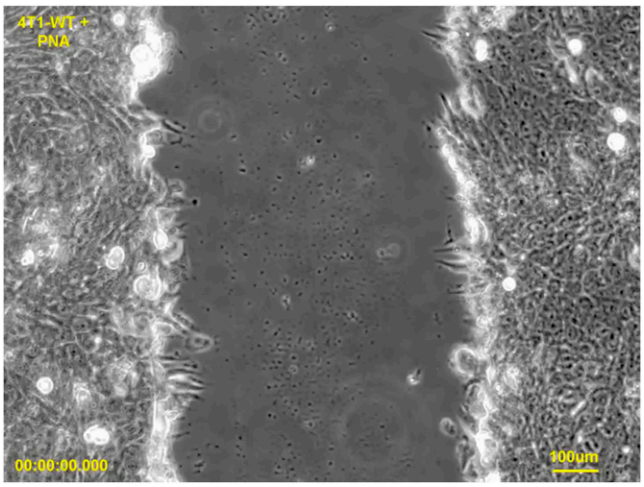

Movie S6. Wild-type 4T1 cells treated with either 40 μg/mL PNA (present movie) or 4 μg/mL VVL do not migrate faster than untreated wild-type 4T1 cells. Frames were acquired at 5-min intervals over an 8-h time period.

Movie S6

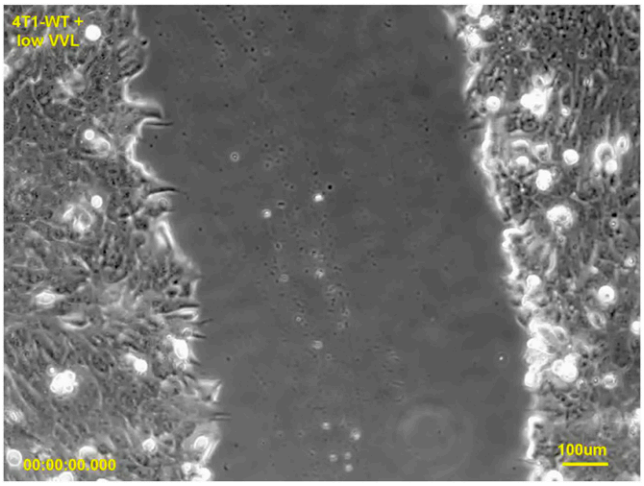

Movie S7. Wild-type 4T1 cells treated with either 40 μg/mL PNA (Movie S6) or 4 μg/mL VVL do not migrate faster than untreated wild-type 4T1 cells. Frames were acquired at 5-min intervals over an 8-h time period.

Movie S7

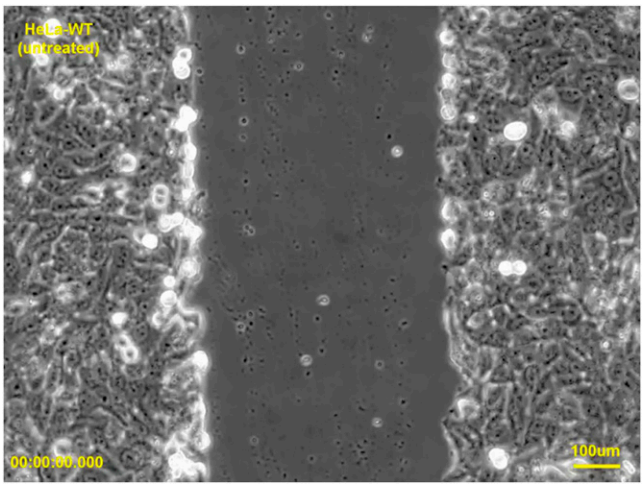

Movie S8. Untreated wild-type HeLa cells (present movie) migrate at a similar rate as 40 μg/mL VVL-treated (Movie S9) or 40 μg/mL PNA-treated cells (Movie S10). Frames were acquired at 5-min intervals over an 8-h time period.

Movie S8

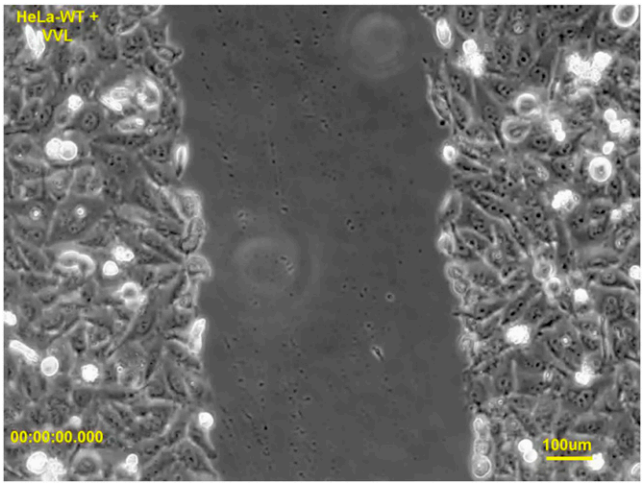

Movie S9. Untreated wild-type HeLa cells (Movie S8) migrate at a similar rate as 40 μg/mL VVL-treated (present movie) or 40 μg/mL PNA-treated cells (Movie S10). Frames were acquired at 5-min intervals over an 8-h time period.

Movie S9

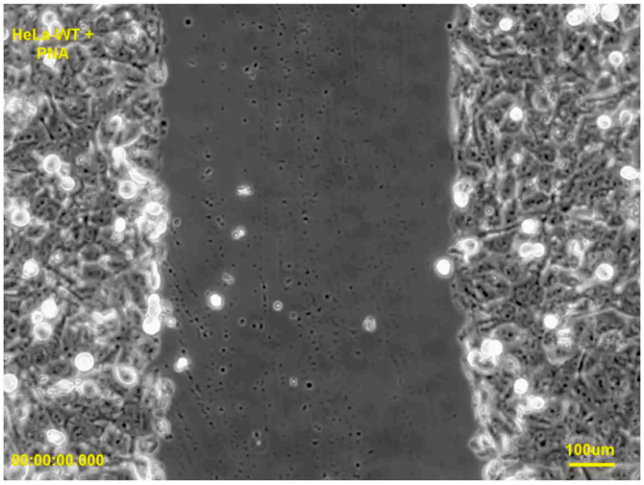

Movie S10. Untreated wild-type HeLa cells (Movie S8) migrate at a similar rate as 40 μg/mL VVL-treated (Movie S9) or 40 μg/mL PNA-treated cells (present movie). Frames were acquired at 5-min intervals over an 8-h time period.

Movie S10

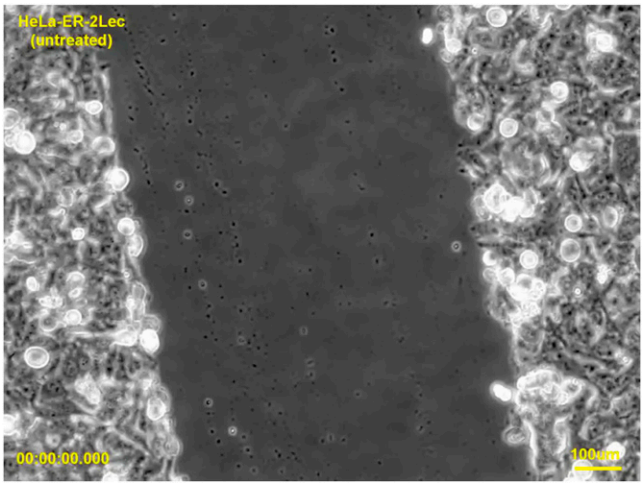

Movie S11. HeLa cells expressing ER-2Lec also migrate at a similar rate as untreated HeLa cells. Frames were acquired at 5-min intervals over an 8-h time period.

Movie S11

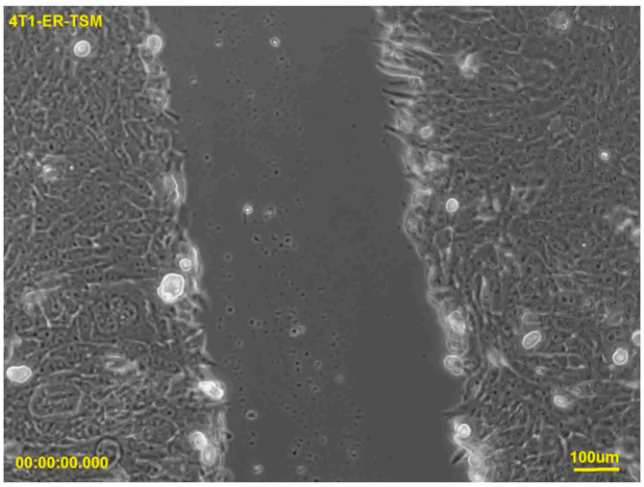

Movie S12. 4T1-ER-TSM cells (present movie) migrate faster than 4T1-ER-2Lec cells (Movie S13) into the denuded area of a scratch wound. Frames were acquired at 5-min intervals over an 8-h time period.

Movie S12

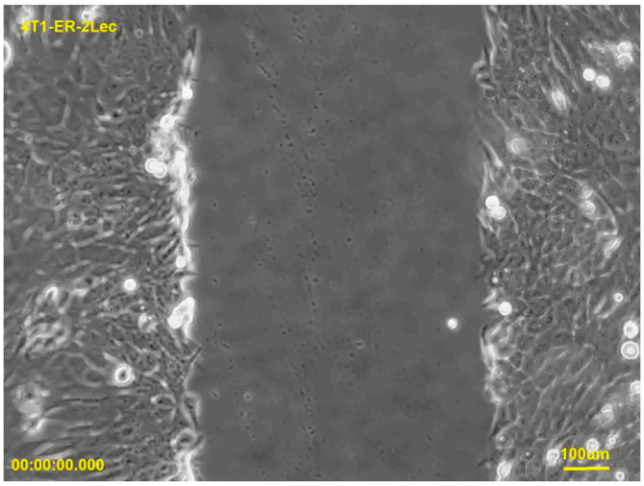

Movie S13. 4T1-ER-TSM cells (Movie S12) migrate faster than 4T1-ER-2Lec cells (present movie) into the denuded area of a scratch wound. Frames were acquired at 5-min intervals over an 8-h time period.

Movie S13

Other Supporting Information Files

Table S1 (DOCX)
Table S2 (DOCX)